

Investigating CM Voltage and Its Measurement for AC/DC Power Adapters to Meet Touchscreen Immunity Requirement

Yiming Li^{1b}, Student Member, IEEE, Shuo Wang^{1b}, Senior Member, IEEE, Honggang Sheng, Choon Ping Chng, and Srikanth Lakshmikanthan

Abstract—The common-mode (CM) noise at the output of ac/dc power adapters can interfere with touchscreen's normal operation in consumer electronic products. Existing power adapter's output CM voltage measurement used in power electronics industry does not align with the touchscreen's sensitivity test used by touchscreen manufacturers. This paper first reviews existing measurement setups and identifies the technical issues in the tests. The CM noise source impedance of ac/dc power adapters and the characteristics of touchscreens are investigated. A new measurement setup is proposed based on both the characteristics of CM noise source of power adapters and touchscreens. A CM voltage limit is also proposed with industry companies. A measurement device is developed for the proposed measurement setup and procedure. The experimental results validate the proposed techniques.

Index Terms—AC/DC power adapters, common-mode (CM) voltage, sensitivity measurement, touchscreen.

I. INTRODUCTION

OVER the last decade, consumer electronic products, such as smartphones, tablets, and laptops, which are integrated with touchscreens have become more and more popular. Under different circumstances, the products are connected to ac/dc power adapters in charging mode when users use the touchscreens. To reduce the cost and size, most of the power adapters with power rating below 75 W employ switching mode flyback converters. These power adapters use two-pronged plugs which have a line prong and a neutral prong but have no safety ground connection as shown in Fig. 1.

The switching operation of semiconductor devices generates high dv/dt . The switching semiconductor devices in the power adapters behave like noise voltage sources. Although the power adapters have an isolation switching transformers for galvanic isolation, there are parasitic capacitances between transformer primary windings and secondary windings, so the output voltages of the power adapters are pulsating. When the users use

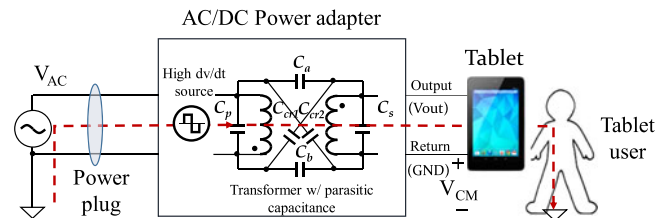


Fig. 1. CM current path including single-phase power line, a power adapter, a touchscreen-enabled device, and a user.

the touchscreens, the displacement currents caused by switching devices' high dv/dt and parasitic capacitance can flow from the primary to the secondary, to the consumer electronic products, to the touchscreens, to the fingers of the users, and to the ground as shown in Fig. 1. The currents finally flow back to the primary of the power converters through the ground.

The displacement currents belong to common-mode (CM) noise currents as they flow between the circuits and the ground. This CM noise has negative impacts to the normal operation of touchscreens.

In the touchscreen industry, the projected-capacitive technology is becoming dominant due to its high durability, excellent optical performance, and the support of unlimited multitouch [1]. Unfortunately, this type of touchscreen is very sensitive to noise. Whenever a product is in charging mode, it is likely that CM noise flowing through the touchscreens will interfere with the normal operation of touch sensors.

A capacitive touchscreen senses the finger touch by sensing the change of electric charge. The CM noise flowing through the touchscreen and human finger can influence the change of electric charge and cause touchscreen malfunction including false touches and jitters.

Power adapter manufacturers have an output CM voltage measurement setup and a test procedure for power adapters to evaluate the CM voltages at the output of the power adapters. Touchscreen manufacturers also have their measurement setup and test procedure to identify the maximum allowable CM voltage on touchscreens. However, these two measurement setups and procedures do not align with each other. The measurement results from power adapters cannot be used to evaluate if the power adapter can meet the immunity requirement of touchscreen manufacturers. Furthermore, the CM currents flowing

Manuscript received December 6, 2017; accepted December 30, 2017. Date of publication February 6, 2018; date of current version February 22, 2018. This work was supported by Google, Inc. (Corresponding author: Shuo Wang.)

Y. Li and S. Wang are with the University of Florida, Gainesville, FL 32611 USA (e-mail: brighturan@ufl.edu; shuo.wang@ece.ufl.edu).

H. Sheng, C. P. Chng, and S. Lakshmikanthan are with Google, Inc., Mountain View, CA 94043 USA (e-mail: honggangs@google.com; choonc@google.com; srikanthl@google.com).

Color versions of one or more of the figures in this paper are available online at <http://ieeexplore.ieee.org>.

Digital Object Identifier 10.1109/TEM.2018.2794318

though the touchscreen are a function of CM noise voltage, noise source impedance, and load impedance, so the CM voltage measurements without correctly considering these parameters cannot be used to accurately evaluate the power adapter and touchscreen systems.

Existing power adapter CM voltage test standard IEC 62684 [2], which is adopted by power electronics industry, specifies the measurement setup and procedure for the measurement of the CM voltage between the output ground (GND) of power adapters and the earth ground. In the setup, the CM impedance between a metal box and the ground is used as the CM noise load of the power adapters. As described previously, the power adapters have CM noise source, source impedance, and CM load impedance which is the CM impedance between the consumer electronic products and the ground. But because the CM load impedance is not equal to the CM impedance between the metal box and the ground specified in IEC 62684, the measured CM voltage is not the actual voltage added to the touchscreen. It means that the standard and the measured CM voltage cannot correctly evaluate if the power adapter can meet the immunity requirement of touchscreens. In order to correctly evaluate if the output CM voltage of power adapters can meet the immunity requirement of touchscreens, the power adapter's CM noise output impedance and the CM load impedance of touchscreens should be investigated in detail.

In this paper, by incorporating the effects of the impedances of touchscreens, a CM voltage measurement setup and procedure are developed for power adapter's CM voltage measurement. A CM voltage limit is also proposed to evaluate if power adapters can meet the immunity requirement of touchscreens.

This paper is organized as follows: In Section II, both existing power adapter's CM voltage test and touchscreen's sensitivity test will be reviewed and the issues will be identified. In Section III, the CM noise model of a flyback converter will be investigated. The CM noise voltage source, CM noise source impedance, and the CM noise propagation paths will be explored. In Section IV, the CM load impedances of the power adapter will be discussed. The most critical CM noise path: from power adapter's output GND, to the touchscreen, to the human body, and to the earth ground, is discussed in detail. The impedances of touchscreens and human bodies are investigated. In Section V, based on the developed CM noise model and the identified critical impedances, a measurement setup is proposed and a measurement device is developed for the proposed measurement setup. A CM voltage limit is identified for power adapters in the proposed measurement setup based on the noise sensitivity test performed on the touchscreen of a Chromebook. In Section VI, experiments are conducted to validate the proposed measurement setup and CM voltage limit.

II. EXISTING NOISE SENSITIVITY TEST FOR TOUCHSCREENS AND CM VOLTAGE MEASUREMENT FOR POWER ADAPTERS

A. Noise Sensitivity Test for Touchscreens

The touchscreen sensitivity test in Fig. 2 [12] is used to find the maximum allowable CM voltage for a specific touchscreen. A voltage with given magnitude and frequency is added between

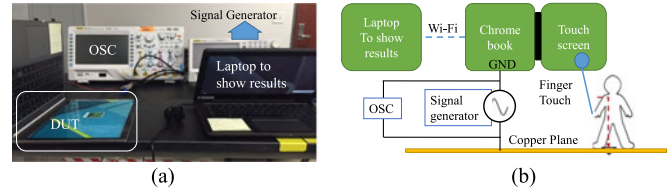


Fig. 2. Noise sensitivity test on a Chromebook: (a) measurement setup and (b) block diagram.

the touchscreen and the ground to emulate the CM voltage added to the touchscreen. If the touchscreen can respond correctly to finger touches, the voltage magnitude will be increased until the touchscreen cannot correctly respond to finger touches. This procedure will be repeated at different frequencies within the concerned frequency range.

In Fig. 2, the device under test is the touchscreen of a Chromebook powered by its own battery. Inside the Chromebook, the GND of the touchscreen is the same as the GND of the Chromebook. A CM voltage with desired magnitude and frequency generated from a signal generator is added between the GND of the Chromebook and a grounded copper plane. An oscilloscope is used to monitor the magnitude of the CM voltage added between the GND and the grounded copper plane. The Chromebook has test software installed and it can wirelessly communicate with a laptop nearby to display the measurement result on the laptop. To exclude the undesired influence from ac grid, the signal generator and the oscilloscope are isolated from ac grid with an isolation transformer. An artificial finger having a fixed touching area with the touchscreen is moved up and down or tapped on the touchscreen to check if the touchscreen can work normally at specific CM voltages. The CM voltage magnitude and frequency can be adjusted for the maximum allowable CM voltage measurement at each frequency within the concerned frequency range. In the measurement, if the touchscreen is able to tolerate a CM voltage level, the CM voltage magnitude will be increased by 1 V until a jitter occurs or the CM voltage reaches the maximum magnitude of the signal generator. The maximum voltage levels that do not cause touchscreen malfunction are recorded for each frequency so the maximum allowable CM voltage limit is identified. All the CM voltages under the maximum allowable CM voltage limit will not cause touchscreen malfunction.

B. Existing Power Adapter CM Voltage Measurement

At present, the standard IEC 62684 [2] is adopted by power electronics industry for power adapter's output CM voltage test. Oscilloscopes are commonly used for CM voltage measurement. The measurement setup is shown in Fig. 3. A 10- Ω resistor load is connected to the power adapter via a 1-m USB cable. A metal box with dimension 10 cm \times 6 cm \times 1.2 cm is connected to the output GND of the power adapter 30 cm above the earth-grounded copper plane to emulate the impedance between the load and the earth. The setup has several issues for touchscreen applications: 1) the metal box may not correctly reflect the actual CM impedance between the consumer electronic products and the ground; 2) the noise from the power grid could

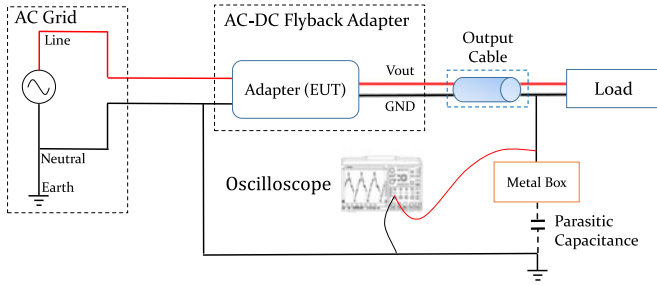


Fig. 3. Existent CM voltage measurement setup.

influence the measurement results; and 3) the characteristics of the oscilloscopes (such as its resolution and probe impedance, etc.) could influence the measurement results.

The measurement setup in Fig. 3 should ensure that the measured CM voltage is the actual voltage added between the Chromebook and the ground in Fig. 2, but the impedance between the metal box and the ground plane is a 50-pF [3] parasitic capacitance. It is not the actual impedance between the Chromebook and the ground. Because of these, the measured CM voltage is not the same CM voltage as added to the touchscreens in the test in Fig. 2. So, the two tests do not align with each other. Furthermore, the CM electromagnetic interference (EMI) noise from the ac power grid can flow to the output of the power adapter, so it can interfere with the measurement result.

Finally, the measured CM voltage at the output of the power adapter has both 50-/60-Hz line frequency voltage and high-frequency CM EMI voltage due to switching operation. The 50-/60-Hz CM voltage is around half of the ac grid voltage, so it is much higher than CM EMI voltage. The oscilloscope has limited resolution so it cannot accurately measure a very small CM EMI voltage superposed on a big 50-/60-Hz CM voltage. In the experiments, even a 12-digit oscilloscope cannot generate satisfactory results. Lin *et al.* [3] proposed to add a high-pass filter to reduce 50-/60-Hz CM voltage, or use a dc source to replace ac grid. These solutions can partially solve the issues somehow, but they make the measurement complicated and may introduce other measurement errors.

Because of these, the measurement setup in Fig. 3 must be improved to solve the related issues and align with the touchscreen’s sensitivity measurement. In the next sections, the CM noise model will be developed for flyback converters. The relationship between the CM voltage added to the touchscreen and the measured CM voltage at the output of the power adapter will be investigated. A measurement setup and a CM voltage limit will be proposed.

III. CM NOISE MODEL OF FLYBACK AC/DC CONVERTERS

A. Flyback Converter and Its Transformer Model

Fig. 4 shows a flyback ac/dc converter popularly used in power adapters connected to ac grid with a two-prong plug. The major CM impedances are also shown in the figure.

In Fig. 4, Z_{Grid} is the impedance between the grid neutral line and the earth ground. It is usually much smaller than other CM impedance in the figure, so it can be ignored in the analysis. An

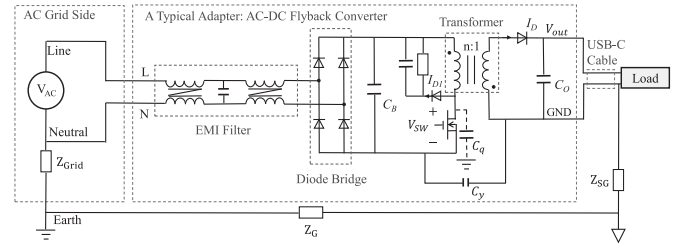


Fig. 4. Flyback ac/dc adapter circuit topology.

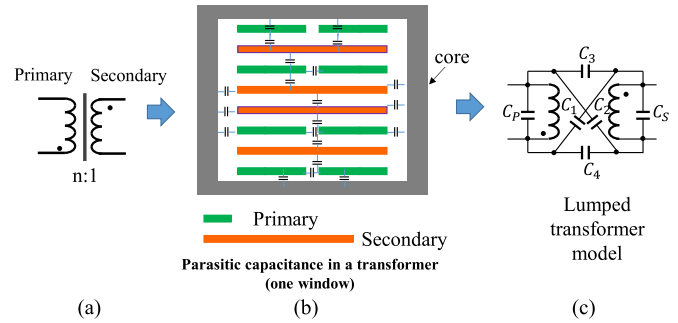


Fig. 5. Transformer parasitic model: (a) ideal transformer model, (b) parasitic capacitance within the transformer, and (c) lumped parasitic transformer model.

EMI filter composed of one big CM inductor, one small inductor, and one DM capacitor is used to attenuate the EMI generated by the flyback converter. The big CM inductor is 27 mH with a 15-pF equivalent parallel capacitance (EPC) and the small CM inductor is 30 μ H with a 6-pF EPC. C_q is the parasitic capacitance between the drain of MOSFET and the earth ground, Z_{SG} is the impedance between the output, which is connected to the load via a USB-C cable, of the power adapter and the earth ground. It is composed of the several impedances including the impedances from output GND to the touchscreen surface and the impedance of human body. C_y is the Y-capacitor across the primary and secondary to reduce CM EMI at the output. Z_G is the impedance of the earth ground.

The transformer of the flyback converter is shown in Fig. 5. Fig. 5(a) shows a transformer with a turn ratio $n:1$ which helps achieve voltage conversion. It also provides galvanic isolation between the primary and the secondary. However, because of the parasitic capacitance, as shown in Fig. 5(b), between the primary and the secondary, and between the windings and the transformer core, the CM EMI can flow from the primary to the secondary. The transformer model can be generally represented with a lumped transformer parasitic model in Fig. 5(c) [5], [6].

B. CM Noise Model and Its Thevenin Equivalent Circuit

To develop a CM noise model for the flyback converter in Fig. 4, based on substitution theory, the MOSFET can be replaced with a voltage source V_{SW} which has the same voltage waveform as the MOSFET drain-to-source voltage and the two diodes can be replaced with current sources I_D and I_{D1} which have the exact same current waveforms as the diode currents [15]. After the substitution, the voltages and currents in the circuit are kept unchanged.

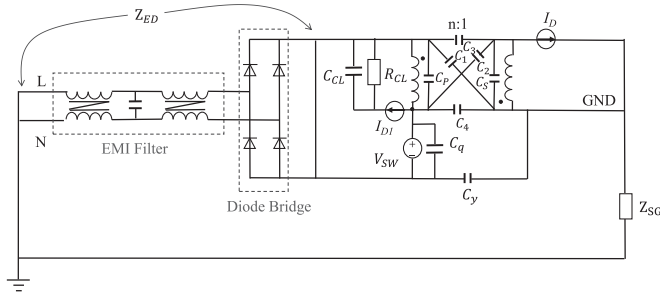


Fig. 6. CM EMI model with nonlinear MOSFET and diodes replaced with voltage and current sources.

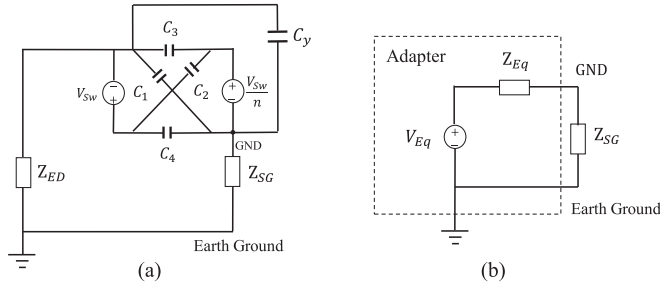


Fig. 7. (a) CM noise model and (b) Thevenin equivalent model.

It should be pointed out that two rules should be followed to apply substitution theory to EMI analysis [7].

- 1) The substitution should avoid voltage-source loops and current-source nodes due to the absence of unique current solutions in voltage-source loops and unique voltage solutions in current-source nodes.
- 2) Although there are different substitutions, the substitutions that are convenient for CM noise analysis are preferred.

The output capacitor C_O and input dc-bus capacitor C_B have very small impedances to EMI noise, so their impedances are ignored. In the CM noise path, the impedances of CM inductors and Z_{SG} are much bigger than Z_{Gid} and Z_G , so Z_{Gid} and Z_G are also ignored for convenience. In many power adapters, MOSFET has no heatsink or its heatsink is connected to the primary GND, so C_q does not contribute to CM noise. Fig. 6 shows the final CM noise model with the transformer replaced with the model in Fig. 5(c).

In Fig. 6, the CM impedance of the EMI filter and the diode bridge can be represented with Z_{ED} . Small Z_{ED} can lead to high CM noise. To investigate the worst scenario, the impedance of the diode bridge can be considered zero. The CM noise generated by V_{SW} , I_D , and I_{D1} can be analyzed based on superposition theory. It is found that I_D and I_{D1} do not contribute to CM noise. Based on network theory, all components in parallel with voltage sources and in series with current sources can be removed. The primary winding capacitance C_P and the secondary winding capacitance C_S are removed because they are in parallel with voltage sources. Fig. 6 can be further simplified to Fig. 7(a). C_1 – C_4 represent the parasitic capacitances between primary and secondary windings of the transformer.

Based on Thevenin theorem, to investigate the CM voltage on Z_{SG} , C_1 to C_4 , C_Y , Z_{ED} , V_{SW} , and V_{SW}/n in Fig. 7(a) can

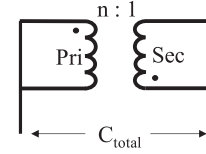


Fig. 8. Measure the total capacitance between the primary and secondary windings.

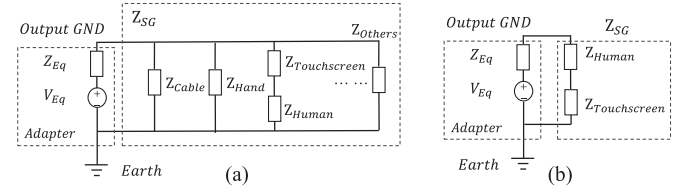


Fig. 9. (a) Impedance Z_{SG} and (b) worst case.

be further reduced to Fig. 7(b). Z_{eq} is the equivalent CM source impedance of the flyback adapter and is given by (1). V_{Eq} is equivalent CM voltage source and is given by (2). In (1) and (2), $C_1 + C_2 + C_3 + C_4$ is the total parasitic capacitance between the primary and the secondary windings. C_1 to C_4 are determined by the winding structure. The total parasitic capacitance can be measured as in Fig. 8. The measured total parasitic capacitance is around 100 pF. $C_1 + C_2 + C_3 + C_4 + C_Y$ is the total capacitance across the primary and the secondary sides. C_Y is 680 pF for the adapter under test.

$$Z_{eq} = \frac{1}{j\omega(C_1 + C_2 + C_3 + C_4 + C_Y)} + Z_{ED} \quad (1)$$

$$V_{eq} = \frac{V_{SW}}{(C_1 + C_2 + C_3 + C_4 + C_Y)} \cdot \left[(C_2 + C_4) - \frac{C_2 + C_3}{n} \right]. \quad (2)$$

The voltage on the touchscreen is part of the voltage on Z_{SG} . If the voltage on Z_{SG} can be reduced, the CM voltage added to the touchscreen can be reduced too.

Based on (2), if condition (3) is met, the CM noise voltage source V_{Eq} will be zero. The CM voltage added to the touchscreen will be zero too

$$(n - 1)C_2 + nC_4 - C_3 = 0. \quad (3)$$

Based on (2), C_1 and C_Y only show up in the denominator of V_{Eq} 's expression because they're across two constant voltage potentials, therefore C_1 and C_Y can help reduce CM voltage. In fact, in Fig. 7(a), C_Y is in parallel with C_1 which indicates they have same influence on CM noise.

IV. INVESTIGATION OF THE IMPEDANCE BETWEEN THE OUTPUT OF POWER ADAPTERS AND THE GROUND

The impedance Z_{SG} from output GND to earth ground is shown in Fig. 9(a). In Fig. 9(a), Z_{SG} consists of several impedances. Z_{Cable} is the impedance between the USB-C cable and the earth ground. The case of the consumer electronic product is usually connected to the GND. Z_{Cable} can be estimated with conductor over ground plane capacitance model and a typical value is 1–10 pF, depending on the cable length, wire gauge,

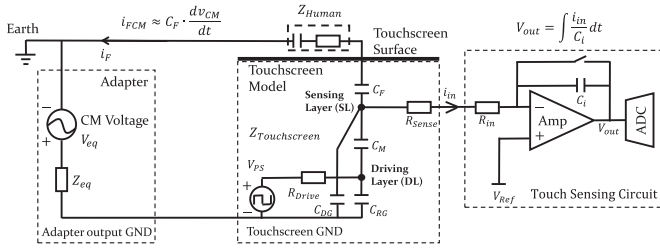


Fig. 10. CM noise model for a projected capacitive touchscreen.

and distance to ground plane. When a user uses the product, Z_{Hand} is the impedance from the output GND to the case of the consumer electronic product, to the hand of the users and to earth ground. The most important path is $Z_{\text{Human}} + Z_{\text{Touchscreen}}$. $Z_{\text{Touchscreen}}$ is the impedance between the output GND and the surface of the touchscreen. Z_{Human} is the impedance from the human fingers to the earth ground via the human body. The CM current flowing through this path influences the normal operation of the touchscreen. Generally, the GND of the touchscreen is directly connected to the adapter's output GND. When a user uses his/her fingers to touch the screen, a small CM current flows from the adapter output GND to the touchscreen surface and then to the earth ground via the human body. Although the CM current is small, it can be detrimental to the touchscreen. Z_{Hand} is usually much smaller than Z_{Cable} (which will be discussed in Section IV-B), so Z_{Cable} 's effect can be ignored. In Fig. 9(a), because Z_{Hand} can help reduce the CM voltage across the touchscreen, when a user holds the product, the touchscreen can work less sensitive to the CM currents. In actual conditions, there may be other parallel impedances in Fig. 9(a). However, because all the impedances parallel with $Z_{\text{Touchscreen}} + Z_{\text{Human}}$ may reduce the CM current flowing through $Z_{\text{Touchscreen}} + Z_{\text{Human}}$ to the earth ground, the worst scenario is when all other impedances are infinite, the CM voltage on the touchscreen reaches the maximum, as shown in Fig. 9(b). In order to investigate the worst case, Z_{Human} and $Z_{\text{Touchscreen}}$ should be investigated.

A. Characteristics of $Z_{\text{Touchscreen}}$

Fig. 10 shows the noise model including power adapter, touchscreen, and touch sensing circuit. Generally, the projected capacitive touchscreen of a consumer electronic product consists of several layers. The top layer (the surface layer) is a glass or plastic cover lens, and it is usually 0.55, 0.75, or 1.1 mm thick [1]. There are two transparent thin-film conductor (ITO) layers, driving layer (DL), and the sensing layer (SL), beneath the touch surface. These layers are separated by a thin-film separator. The ITO layers are electrodes that help sense the capacitance. C_F is the capacitance between the finger on the touchscreen surface and SL. C_{DG} and C_{RG} are parasitic capacitance between ITO layers and the touchscreen GND which is connected to the adapter's output GND. R_{Sense} and R_{Drive} are the resistance of ITO layers which are typically hundreds of Ohms. C_M is the capacitance between SL and DL. A touch sensing circuit connected to the SL can sense the C_M . When the sensing circuit is working, a voltage pulse signal V_{PS} is added to the DL. The current can flow from DL to SL through C_M . Current i_{in} flows

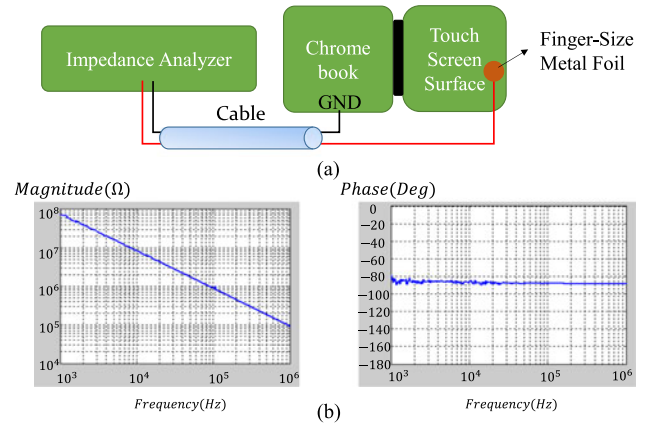


Fig. 11. Measurement of touchscreen's impedance from 1 kHz to 1 MHz: (a) test setup and (b) measurement result.

to the touch sensing circuit for capacitance sensing. When a user's finger touches the screen, if there is no noise interference, a current will flow from SL to the finger through C_F , and then to the earth ground through human body impedance. As a result, the current i_{in} changes and the capacitance sensed by the touch sensing circuit changes, so the touch is recognized. The control circuit will continuously scan the touch sensing grid on the touchscreen at certain frequencies. So, a finger touch can always be recognized on the touchscreen.

If the output of a power adapter has CM noise voltage and part of it is added to the touchscreen, the current i_{in} will be influenced by the CM voltage and the touch sensing circuit may not work properly. Obviously, C_F is approximately proportional to the touching area. Fig. 11(a) shows the measurement setup of $Z_{\text{Touchscreen}}$. To guarantee all the measurements can generate repeatable results, a piece of round shape metal foil with a diameter equal to 12 mm is used to emulate the touching area of a finger [12]. The impedance $Z_{\text{Touchscreen}}$ between the GND of the touchscreen and the metal foil was measured using an impedance analyzer from 1 kHz to 1 MHz because within this range the touchscreen is sensitive to the noise. The measured impedance is shown in Fig. 11(b). It is a pure capacitance with a value of 1.6 pF.

B. Characteristics of Z_{Human}

For the human body impedance Z_{Human} , the impedance between the finger of a human and a metal plate on which the human was standing on was measured using an impedance analyzer. The measurement setup is shown in Fig. 12(a) and the result is shown in Fig. 12(b).

The measurement result shows that Z_{Human} is capacitive but is much smaller than touchscreen's impedance. Since Z_{Human} and $Z_{\text{Touchscreen}}$ are in series, Z_{Human} can be ignored.

Based on the measurement and analysis above, the impedance from power adapter's output GND to the earth ground can be modeled as a 1.6-pF small capacitance in this case. Considering the worst scenario, all the impedances parallel with $Z_{\text{Touchscreen}} + Z_{\text{Human}}$ in Fig. 9(a) can be ignored so the CM voltage added to the touchscreen reaches the maximum. Because of this, Z_{SG} can be modeled with $Z_{\text{Touchscreen}}$.

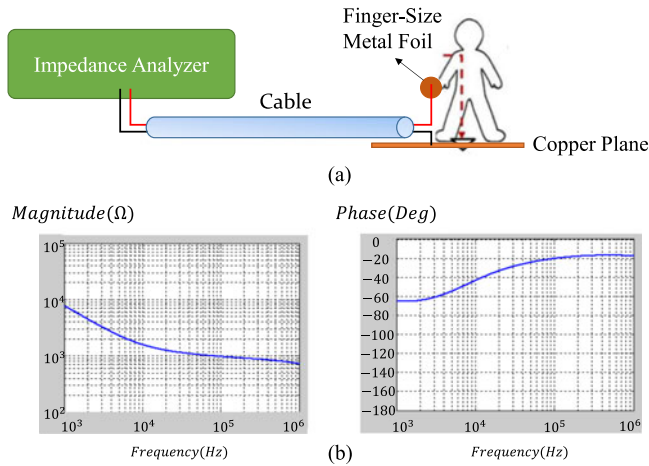


Fig. 12. Measurement of human body impedance from 1 kHz to 1 MHz: (a) test setup and (b) measurement result.

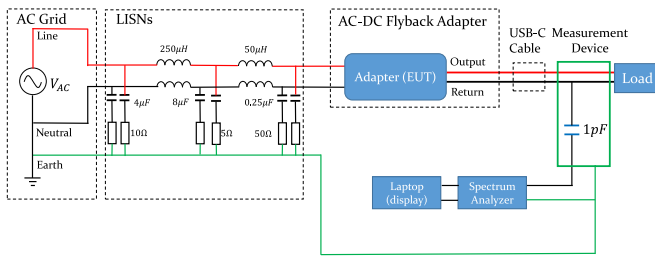


Fig. 13. Proposed CM voltage measurement setup for ac/dc power adapters.

It should be noted that Z_{Hand} can be measured in a similar way. Based on the measurement result, Z_{Human} and Z_{Hand} are in the same order of magnitude, which is much lower than $Z_{\text{Touchscreen}}$. It also explains that when a user holds the product, the CM current will bypass by Z_{Hand} and the touchscreen can work less sensitive to the CM noise.

V. PROPOSED CM VOLTAGE MEASUREMENT SETUP AND DISCUSSION

An oscilloscope's voltage probe has input impedance (8 pF//10 MΩ as defined in IEC 62684) whose magnitude could be comparable to or even smaller than Z_{SG} which is determined by the $Z_{\text{Touchscreen}}$, a 1.6-pF capacitance, so if the probe is used to measure the CM voltage between the output GND and the ground, the probe's impedance will be in parallel with Z_{SG} . This results in a greatly reduced impedance. Because the equivalent noise source impedance Z_{Eq} in Fig. 7(b) is determined by the parasitic capacitance between transformer's primary and the secondary windings and the impedance Z_{ED} . Z_{ED} is mostly determined by the big CM inductor within the concerned frequency range from 1 kHz to 1 MHz. Based on the parameters of the big CM inductor in Section III-A, its impedance is comparable to the input impedance of voltage probe, so the probe impedance may greatly reduce the measured CM voltages. Because of this, oscilloscopes should not be directly used to measure the CM voltages between the output GND and the ground.

A CM voltage measurement setup is proposed in Fig. 13 with a spectrum analyzer and a developed measurement device

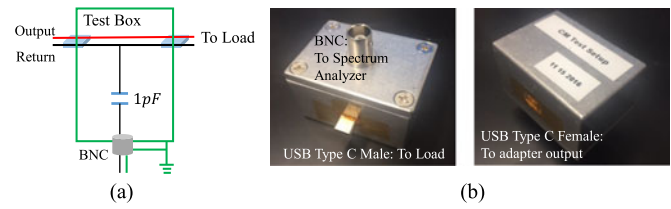


Fig. 14. Prototype of the developed measurement device to help perform CM voltage measurement: (a) circuit and (b) prototype.

for power adapter manufacturers without using any touchscreen enabled electronic products as its load.

In Fig. 13, line impedance stabilization networks (LISNs) are used between the power grid and the power adapter to isolate the noise from power grid. A circuit breaker is connected between LISNs and the power adapter. A measurement device in Fig. 14 has been developed to help conduct CM voltage measurements in Fig. 13.

In Fig. 14, the measurement device has a USB-C female input power port, which will be connected to the output of the power adapter, a USB-C male output power port, which will be connected to a load resistor, and a BNC output port which will be connected to a spectrum analyzer. The devices can have different power connectors depending on the actual connectors used in power adapters. Inside the shielded metal box is a 1-pF capacitor which is connected between the output GND of the power adapter and the spectrum analyzer. The 1-pF capacitor is used to emulate the capacitance of touchscreen. Since the capacitance of touchscreens is typically from 1 to 3 pF [12], a 1-pF capacitor can emulate the worst scenario as it leads to the highest CM voltage. A different capacitance can also be used to emulate touchscreen's capacitance depending on the actual touchscreen used. The spectrum analyzer, measurement device, and LISNs are grounded as shown in Fig. 13. Because the parasitic capacitance between the load and the ground is in parallel with the 1-pF capacitor and it will reduce the measured CM voltage, no ground plane should be used in the setup so the parasitic capacitance between the load and the ground can be minimized. There should have no big pieces of metal near the load so the parasitic capacitance between the load and the ground can be minimized. The load resistor should have enough distance to the measurement device so the parasitic capacitance between the load resistor and the metal box of the measurement device can be minimized too.

In Fig. 13, since the input impedance of the spectrum analyzer is constant 50 Ω which is much smaller than the emulated touchscreen capacitance, the CM current flowing through spectrum analyzer is determined by the 1-pF capacitor only. With the measured CM voltages on the spectrum analyzer, the CM current flowing through the 1-pF capacitor and the CM voltage on the 1-pF capacitor can be calculated.

Another advantage of this setup is that since the 1-pF capacitor has a large impedance at low frequencies, the line-frequency component in the CM current is greatly reduced. There is no inference from line frequency CM current component as in Fig. 3 so the result is more accurate.

Since the line-frequency CM voltage at power adapter's output can reach half of the ac line voltage magnitude [13], the

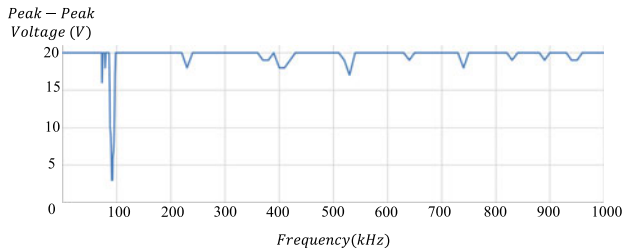


Fig. 15. Single-finger touch CM voltage limit derived from the experiments in Fig. 2.

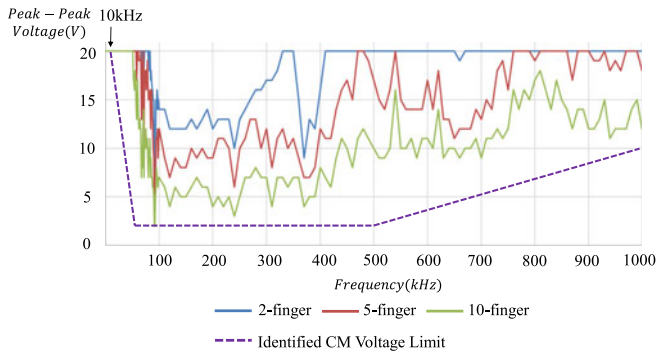


Fig. 16. Multifinger touch CM voltage limits derived from the experiments in Fig. 2.

voltage rating of the capacitor can be selected as 200 V/400 V ac for 110 V/220 V ac system.

Unlike the existing measurement setup in Fig. 3, the measurement setup in Fig. 13 correctly includes the touchscreen's CM impedance, and the CM voltage limit for the output of the power adapter can therefore be derived based on touchscreen's sensitivity test in Fig. 2. Since the human body impedance is negligible, as shown in Fig. 2, the CM voltage on the touchscreen is equal to the output voltage of the signal generator as discussed in Section IV. In Fig. 13, if the measured CM voltage is below the CM voltage limit, the touchscreen can perform properly. If the measured CM voltage is higher than the limit, jitters or false touches may occur. Fig. 15 shows the CM voltage limit derived from the experiments in Fig. 2 for single-finger touch on a Chromebook's touchscreen. Similarly, multi-finger touch tests can be performed in the measurement setup in Fig. 2 and the CM voltage limits for 2-finger, 5-finger and 10-finger can be identified in Fig. 16.

Most of touchscreens support multitouch. The worst scenario happens at ten-finger touch as the highest CM current will flow through C_F in Fig. 10, causing touch sensing circuit malfunction. Because of this, the CM voltage limit should be determined based on ten-finger touch measurement result in Fig. 16. The dash line in Fig. 16 is the finally identified CM voltage limit based on the green-line ten-finger measurement result. (Note: in this case, C_F may be higher than that in single-finger touch, nevertheless, with a 1-pF emulation cap, when the noise is lower than the limit, it ensures that there will not be malfunction problem for both single-finger and multifinger touch, which simplifies the test procedure.)

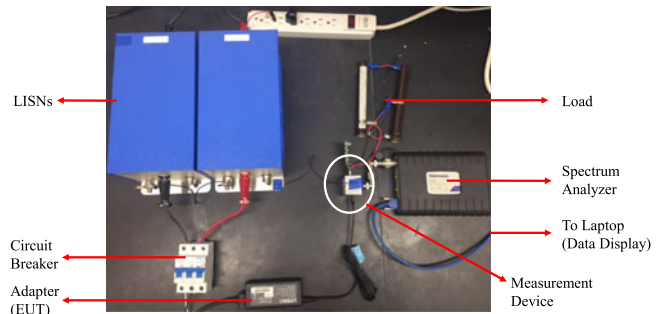


Fig. 17. CM voltage measurement setup with the developed measurement device.

Appropriate voltage margin is used when determine this voltage limit. There is only a very small voltage margin around 90 kHz because the measured problematic CM voltage is already very small: around 2 V peak-peak.

The identified limits for the CM voltage on the touchscreen in Fig. 16 can be further converted to the limits for the CM voltage measured on the spectrum analyzer in Fig. 13. With the converted CM voltage limit, the measured CM voltage on the spectrum analyzer in Fig. 13 can be directly used to determine whether the CM voltage of the adapter can meet the touchscreen's CM voltage limits.

Based on Fig. 13, the conversion equation between two voltage limits is derived as follows:

$$V_{SP} = 20 \cdot \log_{10} \left(\frac{V_{CM}}{2\sqrt{2}} \cdot 50 \cdot 2\pi f C \right) + 120 \quad (\text{dB} \cdot \mu\text{V}) \quad (4)$$

where V_{CM} is the CM voltage limit identified in the experiment of Fig. 2 and its unit is volt. Since the V_{CM} in Figs. 15 and 16 is peak-peak value and the result of spectrum analyzer is based on the RMS value, V_{CM} needs be converted to RMS value as shown in (4). C is the emulation capacitance in the developed measurement device. V_{SP} is the converted CM voltage limit. The input impedance of the spectrum analyzer is 50 Ω . The unit of V_{SP} is dB $\cdot\mu$ V.

VI. EXPERIMENTAL VERIFICATION AND DISCUSSION

The actual measurement setup same as that in Fig. 13 is shown in Fig. 17. The ac input of the power adapter is connected to a 110 V/60 Hz ac systems via LISNs and a circuit breaker. The dc output of the adapter is connected to a power resistor via the developed measurement device. A laptop is used to process the data collected by a portable spectrum analyzer. The laptop is powered by its battery to minimize external noise. As discussed previously, no ground plane should be used so the parasitic capacitance between the output GND and the ground can be minimized. The metal box of measurement device, the shielding of the BNC connector, and the ground of LISNs are connected to the earth ground via wires as shown in Fig. 17.

In the experiments, the resolution bandwidth (RBW) of the spectrum analyzer is set to 200 Hz. 200 Hz is chosen because of the fact that large RBW can introduce high background noise

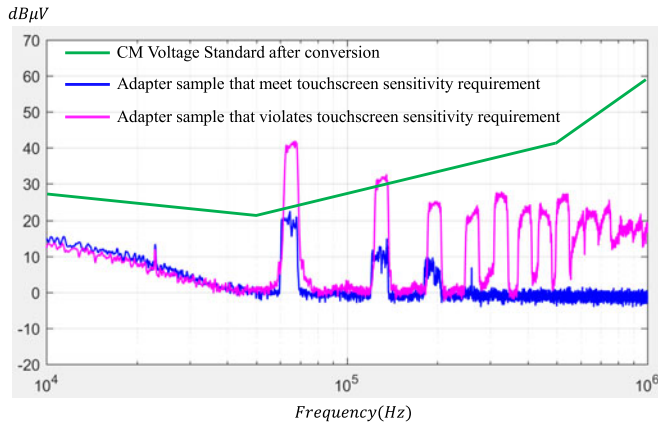


Fig. 18. CM voltage test result for adapter samples with ten-finger touch.

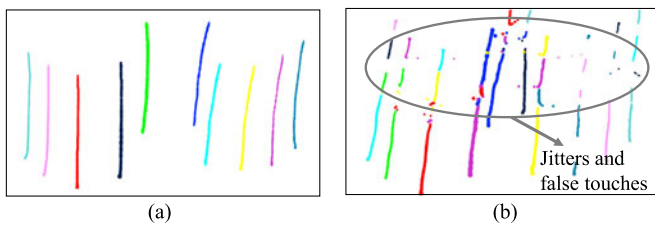


Fig. 19. Noise sensitivity test result for adapters: (a) example of meeting touchscreen sensitivity requirement and (b) example of violating touchscreen sensitivity requirement.

which may interfere with the measured CM voltage. The average detector was used in the spectrum analyzer because in noise sensitivity test, the obtained V_{CM} can be regarded as an average of maximum allowable voltage levels. The measured results for the worst scenario, ten-finger touch, are shown in Fig. 18 as an example.

Fig. 18 shows the measured CM noise voltage. The green line represents the converted CM voltage limit. The blue curve shows the measured CM voltage of a qualified adapter. It is lower than the limit. The pink curve shows the measured CM voltage of an unqualified adapter. It does not meet the limit.

To validate the developed technique and the measurement results in Fig. 18, touchscreen's sensitivity test was conducted in Fig. 19. Fig. 19(a) and (b) shows the ten-finger touch sensitivity test results for the qualified adapter and the unqualified adapter, as used in the measurement in Fig. 18. It is shown that with the qualified adapter, the touchscreen has no jitters or false touch observed, while for the unqualified adapter, there are jitters and false touches observed on the touchscreen.

For the touchscreens supporting less than ten-finger touch, the worst scenario always happens when most of fingers touch the screens. The CM voltage limits can be determined similarly to that in Fig. 16 and the sensitivity can be tested similarly to the ten-finger touch test in this section.

It should be pointed out that the goal of the proposed measurement setup in Fig. 13 is not to precisely measure the CM voltage in the whole frequency range. The objective is to check whether an adapter causes touchscreen malfunction. The proposed setup meets this goal.

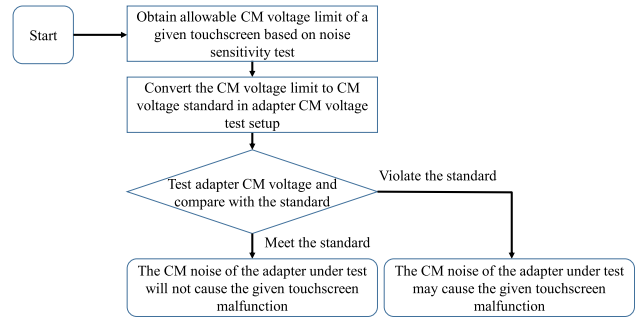


Fig. 20. Flowchart of the proposed test procedure.

Based on (4), the accuracy of the tested results based on the proposed setup will be influenced by the error from the spectrum analyzer and the tolerance of emulation capacitor. Also, the parasitic capacitance which is in parallel with the emulation capacitor will influence the result. Therefore, it should be minimized as discussed above.

Fig. 20 shows a flowchart of the proposed algorithm. The improvements over conventional test setup are summarized as follows.

- 1) The result with conventional CM voltage test setup does not align with the noise sensitivity measurement result of a touchscreen, whereas the proposed method can.
- 2) The conventional test setup uses a 50-pF capacitance which is much different from touchscreen impedance, whereas the proposed setup emulates it with a 1-pF capacitor which is much more accurate.
- 3) The conventional test setup uses an oscilloscope to measure the CM voltage but its characteristics such as resolution and probe impedance, etc., will influence the measurement, while the proposed method uses a spectrum analyzer and these problems can be avoided.
- 4) In conventional test setup, the noise from the ac grid will influence the measurement, while the proposed method employs LISNs to eliminate the ac grid noise.

VII. CONCLUSION

The paper first reviewed the existing noise sensitivity test technique for touchscreens and CM voltage measurement technique for power adapters. It was found that the existing CM voltage measurement technique for power adapters does not align with the touchscreen noise sensitivity test technique. To solve this issue, this paper analyzed the CM voltage model for a typical flyback adapter and discussed its equivalent impedance for CM noise. The impedance of touchscreen, human impedance, and the equivalent impedance from the adapter output GND to the earth ground were also discussed in detail. Based on the investigation, a small, but reasonable capacitor was used to emulate the impedance between the adapter's output GND and the ground in the experiments. Based on the research, a new CM voltage measurement setup and a measurement device were proposed for ac/dc power adapters. The CM voltage limit was also derived for the proposed measurement setup. Finally, the noise sensitivity test was performed on a touchscreen-enabled Chromebook. Experiment results validated the developed technique.

REFERENCES

- [1] G. Barret and R. Omote, "Projected-capacitive touch technology," *Inf. Display*, vol. 26, no. 3, pp. 16–21, Mar. 2010.
- [2] *Interoperability Specifications of Common External Power Supply (EPS) for Use With Data-Enabled Mobile Telephones*, IEC Standard 62684, 2011.
- [3] R. L. Lin, J. Y. Guo, and C. M. Chang, "Study of common-mode voltage measurements for IEC62684," *IEEE Trans. Ind. Appl.*, vol. 50, no. 5, pp. 2976–2984, Sep./Oct. 2014.
- [4] D. Cochrane, D. Y. Chen, and D. Boroyevic, "Passive cancellation of common-mode noise in power electronic circuits," *IEEE Trans. Power Electron.*, vol. 18, no. 3, pp. 756–763, May 2003.
- [5] P. Kong, S. Wang, and F. C. Lee, "Reducing common mode EMI noise in two-switch forward converter," in *Proc. 2009 IEEE Energy Convers. Congr. Expo.*, San Jose, CA, USA, 2009, pp. 3622–3629.
- [6] B. G. Kang, S. K. Chung, J. S. Won, and H. S. Kim, "EMI reduction technique of flyback converter based on capacitance model of transformer with wire shield," in *Proc. 2015 9th Int. Conf. Power Electron. ECCE Asia*, Seoul, South Korea, 2015, pp. 163–169.
- [7] Y. Chu and S. Wang, "A generalized common-mode current cancellation approach for power converters," *IEEE Trans. Ind. Electron.*, vol. 62, no. 7, pp. 4130–4140, Jul. 2015.
- [8] L. Xie, X. Ruan, and Z. Ye, "Equivalent noise source: An effective method for analyzing common-mode noise in isolated power converters," *IEEE Trans. Ind. Electron.*, vol. 63, no. 5, pp. 2913–2924, May 2016.
- [9] Q. Chen, W. Chen, Q. Song, and Z. Yongfa, "An evaluation method of transformer behaviors on common-mode conduction noise in SMPS," in *Proc. 2011 IEEE 9th Int. Conf. Power Electron. Drive Syst.*, Singapore, 2011, pp. 782–786.
- [10] P. Meng, J. Zhang, H. Chen, Z. Qian, and Y. Shen, "Characterizing noise source and coupling path in flyback converter for common-mode noise prediction," in *Proc. 2011 26th Annu. IEEE Appl. Power Electron. Conf. Expo.*, Fort Worth, TX, USA, 2011, pp. 1704–1709.
- [11] H. I. Hsieh, L. Huwang, T. C. Lin, and D. Chen, "Use of a Cz common-mode capacitor in two-wire and three-wire offline power supplies," *IEEE Trans. Ind. Electron.*, vol. 55, no. 3, pp. 1435–1443, Mar. 2008.
- [12] H. W. Klein, "Noise immunity of touchscreen devices," White Paper, Feb. 2013.
- [13] Y. Li, S. Wang, H. Sheng, S. Lakshminathan, and C. P. Chng, "Investigation and reduction of line frequency common mode voltages at the outputs of AC/DC power converters," in *Proc. IEEE Int. Symp. Electromagn. Compat. Signal Power Integrity*, Washington, DC, USA, Aug. 7–11, 2017, pp. 364–369.
- [14] A. A. Worshevsky and R. L. Patlatiy, "Generation of low frequency common mode voltages in secondary supply units," in *Proc. 2007 7th Int. Symp. Electromagn. Compat. Electromagn. Ecol.*, Saint-Petersburg, Russia, 2007, pp. 67–69.
- [15] S. Wang, P. Kong, and F. C. Lee, "Common mode noise reduction for boost converters using general balance technique," *IEEE Trans. Power Electron.*, vol. 22, no. 4, pp. 1410–1416, Jul. 2007.
- [16] H. Zhang and S. Wang, "Two-capacitor transformer winding capacitance models for common mode EMI noise analysis in isolated DC-DC converters," in *Proc. 2016 IEEE Energy Convers. Congr. Expo.*, 2016, pp. 1–8.



Yiming Li (S'16) received the B.S.E.E. degree in electrical engineering from Zhejiang University, Zhejiang, China, in 2015, and is currently working toward the Ph.D. degree at the University of Florida, Gainesville, FL, USA.

His research interests include electromagnetic interference/compatibility in power electronic systems. He is also studying on transformer and EMI filter design and optimization for switching mode power supplies.

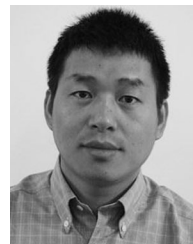


Shuo Wang (S'03–M'06–SM'07) received the Ph.D. degree in electrical engineering from Virginia Tech, Blacksburg, VA, USA, in 2005.

He has been an Associate Professor with the Department of Electrical and Computer Engineering, University of Florida, Gainesville, FL, USA, since 2015. From 2010 to 2014, he was with the University of Texas at San Antonio, TX, USA, first as an Assistant Professor and later as an Associate Professor. From 2009 to 2010, he was a Senior Design Engineer with GE Aviation Systems, Vandalia, OH, USA.

From 2005 to 2009, he was a Research Assistant Professor with Virginia Tech. He has authored/coauthored more than 150 IEEE journal and conference papers and holds eight US patents.

Dr. Wang is an Associate Editor for the IEEE TRANSACTIONS ON INDUSTRY APPLICATIONS and a Technical Program Co-Chair for IEEE 2014 International Electric Vehicle Conference. He was a recipient of the Best Transaction Paper Award from the IEEE Power Electronics Society in 2006 and two William M. Portnoy Awards for the papers published in the IEEE Industry Applications Society in 2004 and 2012. He was also a recipient of the prestigious National Science Foundation CAREER Award in 2012.



Honggang Sheng received the B.S. degree from Xi'an Jiaotong University, Xi'an, China, in 1998, the M.S. degree from the South China University of Technology, Guangzhou, China, in 2003, and the Ph.D. degree from Virginia Polytechnic Institute and State University (Virginia Tech), Blacksburg, VA, USA, in 2009, all in electrical engineering.

Since 2011, he has been with Google, Inc., Mountain View, CA, USA, as a Power Engineer for the data center and consumer hardware.



Choon Ping Chng received the B.S.E.E. degree from the University of Denver, Denver, CO, USA, in 1997, and the M.S.E.E. degree from Stanford University, Stanford, CA, USA, in 1999, all in electrical engineering (VLSI design).

He has been a Staff Hardware Engineer with Google, Inc., Mountain View, CA, USA, since 2010, where he was involved in the creation of Chromebooks. He is currently in charge of Hangouts Meet hardware development at Google, Inc.



Srikanth Lakshminathan has been with Google, Inc., Mountain View, CA, USA, as a Staff Hardware Engineer and led power design solutions in multiple product areas including data center and Chrome Hardware from 2006. He has been the Technical Power Team Manager with Google Hardware PA since 2016.